Research Square

Preprints are preliminary reports that have not undergone peer review.
They should not be considered conclusive, used to inform clinical practice,
or referenced by the media as validated information.

The semi-dwarfing gene Rht-dp from dwarf Polish wheat (Triticum polonicum L.) is the “Green Revolution” gene Rht-B1b

Songyue Chai
Triticeae Research Institute, Sichuan Agricultural University
Qin Yao
Triticeae Research Institute, Sichuan Agricultural University
Xu Zhang
Triticeae Research Institute, Sichuan Agricultural University
Xue Xiao
Triticeae Research Institute, Sichuan Agricultural University
Xing Fan
Triticeae Research Institute, Sichuan Agricultural University
Jian Zeng
College of Resources, Sichuan Agricultural University
Lina Sha
Triticeae Research Institute, Sichuan Agricultural University
Houyang Kang
Triticeae Research Institute, Sichuan Agricultural Universitu
Haiqin Zhang
Triticeae Research Institute, Sichuan Agricultural University
Jun Li
Crop Research Institute, Sichuan Academy of Agricultural Sciences
Yonghong Zhou
Triticeae Research Institute, Sichuan Agricultural University
Yi Wang (wangyi@sicau.edu.cn)
Triticeae Research Institute, Sichuan Agricultural University

Research article

Keywords: Dwarf Polish wheat, homologous cloning, molecular mapping, Rht-B1b, RNA-seq

Posted Date: January 12th, 2021

DOI: https://doi.org/10.21203/rs.3.rs-60100/v3

License: This work is licensed under a Creative Commons Attribution 4.0 International License.
Read Full License

Version of Record: A version of this preprint was published on January 19th, 2021. See the published version at https://doi.org/10.1186/s12864-021-07367-x.

Abstract

Background: The wheat dwarfing gene increases lodging resistance, the grain number per spike and harvest index. Dwarf Polish wheat (*Triticum polonicum* L., 2n = 4x = 28, AABB, DPW), initially collected from Tulufan, Xinjiang, China, carries a semi-dwarfing gene *Rht-dp* on chromosome 4BS. However, *Rht-dp* and its dwarfing mechanism are unknown.

Results: Homologous cloning and mapping revealed that *Rht-dp* is the 'Green Revolution' gene *Rht-B1b*. A haplotype analysis in 59 tetraploid wheat accessions showed that *Rht-B1b* was only present in *T. polonicum*. Transcriptomic analysis of two pairs of near-isogenic lines (NILs) of DPW×Tall Polish wheat (*Triticum polonicum* L., 2n = 4x = 28, AABB, TPW) revealed 41 differentially expressed genes (DEGs) as potential dwarfism-related genes. Among them, 28 functionally annotated DEGs were classed into five sub-groups: hormone-related signalling transduction genes, transcription factor genes, cell wall structure-related genes, reactive oxygen-related genes, and nitrogen regulation-related genes.

Conclusions: These results indicated that *Rht-dp* is *Rht-B1b*, which regulates pathways related to hormones, reactive oxygen species, and nitrogen assimilation to modify the cell wall structure, and then limits cell wall loosening and inhibits cell elongation, thereby causing dwarfism in DPW.

Background

Plant height is an important agronomic trait of crops. The discovery and utilization of semi-dwarfing genes in rice (*Oryza sativa*) and wheat (*Triticum aestivum*) triggered the "Green Revolution", as dwarfism not only improves lodging resistance [1], but also increases the grain number per spike and harvest index [2-3]. Increasing numbers of dwarf varieties of crops are being bred for production [4], and the dwarfing mechanisms in many crops are clearly revealed [5-7].

In wheat, 27 dwarfing genes including 32 alleles are present on chromosomes 2A, 2B, 2D, 3B, 4B, 4D, 5A, 5D, 6A, 7A, and 7B [8-16]. Twenty-two of those genes were discovered from hexaploid wheat, including *Rht1* (*Rht-B1b*), *Rht2* (*Rht-D1b*), *Rht8*, and *Rht12.* Those genes are widely utilized to breed new cultivars while only *Rht1* and *Rht2* have been cloned [6, 17-18]. As the parent of hexaploid wheat, tetraploid wheat owns many dwarfing genes, for example, *Rht14*, *Rht15*, *Rht16*, *Rht18*, *Rht19,* and *Rht-R107* in *Triticum durum* [19-20], *Rht22* in *T. turgidum* [21], contains *Rht-B1f* in *T. aethiopicum* [15], and *Rht-B1*^{IC12196} and *Rht-dp* in *T. polonicum* [10, 14]. Due to *T. polonicum* has a high 1000-grain weight and accumulates high concentrations of zinc and iron in grains, it is recommended to be a valuable material for wheat genetic improvement [22]. However, the details of its dwarfing genes, *Rht-dp* and *Rht-B1*^{IC12196}, are still unknown.

As a gibberellin (GA)-insensitive semi-dwarfing gene, *Rht-dp* was identified from dwarf polish wheat (DPW, *T. polonicum*) originally collected from Tulufan, Xinjiang province, China [10, 23]. Transcriptomic and proteomic analyses suggested that *Rht-dp* is probably involved in the phenylpropanoid pathway. It was found to reduce the contents of lignin, cellulose, and S-adenosyl-methionine, and increase the contents of flavonoids, which ultimately limits cell expansion and causes dwarfism [24]. Although those

results indicated the potential mechanism of *Rht-dp*, the candidate gene of *Rht-dp* remained unknown. Genetic analysis of F_2 population derived from the cross of DPW and tall Polish wheat (TPW) indicated that *Rht-dp* should be a recessive gene [10]. However, the separated threshold of plant height was significant larger than the plant height of DPW [10, 23], which implied that the effect of *Rht-dp* on reducing plant height might be partially covered by one or more non-allelic loci. Further study mapped *Rht-dp* onto chromosome 4BS between the SSR markers *Xgpw3017* and *Xwmc511*, and suggested that *Rht-dp* may be an alternative allele at the *Rht-B1* locus [10]. However, due to the limited numbers of F_2 plants and molecular markers used in the analysis, a genomic alignment against the genome of *Triticum aestivum* 'Chinese Spring' (IWGSC RefSeq v1.0) (International Wheat Genome Sequencing Consortium, 2018) indicated that the region between *Xgpw3017* and *Xwmc511* did not include the *Rht-B1* locus. Additionally, *Rht-B1b* and its alleles are semi-dominant genes [6, 25-26]. Thus, we can't confirm whether *Rht-dp* is *Rht-B1b* or its allele, or a new gene.

Rht-B1b encodes a premature DELLA protein, which prevents GID1 from binding to its target [12]. The premature DELLA protein truncates the GA response, resulting in dwarfism. *Rht-B1b* originates from the native Japanese dwarf variety 'Norin 10' [27]. However, it was successfully transferred from 'Norin 10' to 'Cando' in the 1960s and widely used in durum wheat breeding [28]. Meanwhile, three alleles of *Rht-B1b*, *Rht-B1f*, *Rht-R107,* and *Rht19*, were also discovered from *T. aethiopicum* and *T. durum*, respectively [15, 19]. Although DPW is originally collected from Tulufan, Xingjiang, China [23] and the progenitor of *T. polonicum* is neither 'Norin 10', *T. aethiopicum* nor *T. durum* [10, 29], we still hypothesized that the candidate gene of *Rht-dp* may be *Rht-B1b* or its one of alleles, because only *Rht-B1b* and its alleles as dwarfing genes have been found on 4BS to date [10, 23, 28, 30].

To test this hypothesis and to understand the dwarfing mechanism of *Rht-dp* in DPW, we firstly cloned *Rht-B1* to investigate sequence differences in *Rht-B1* between DPW and TPW. Secondly, we developed and applied a specific molecular marker of *Rht-B1* and SSR markers on 4BS to genetically confirm the candidate region using three recombinant inbred lines (RILs). Thirdly, two pairs of near-isogenic line (NIL) obtained from the F_7 population of DPW×TPW were conducted transcript analyses to reveal the molecular mechanism of *Rht-dp*; meanwhile, F_1 plants and a F_2 population derived from the cross of a pair of NIL were developed for further genetic analysis. Finally, we conducted a haplotype analysis of *Rht-dp* to reveal the natural distribution among 59 tetraploid wheat accessions.

Methods

Plant materials and growth conditions

The DPW and TPW lines were originally collected from Tulufan, Xinjiang province, China, by Prof. Chi Yen and Junliang Yang (Sichuan Agricultural University, China) in the 1980s. The F_1 population of DPW×TPW and the F_2 population (401 plants) derived from DPW×TPW were individually developed for trait investigation. Two RIL populations (F_7 including 330 lines and F_8 including 300 lines) derived from DPW×TPW, and a RIL population (F_6 including 194 lines) derived from DPW×Jianyangailanmai (AABB, 2n

= 4x = 28, *T. turgidum* L., Ailanmai), were developed for gene mapping. Two pairs of NILs (D_60/T_58, and D_33/T_35, D and T represent dwarf and tall phenotype, respectively) derived from two heterozygous F_7 lines were selected for transcript analyses. Meanwhile, F_1 plants and a F_2 population (244 plants) derived from the cross of D_60 and T_58 were developed for trait investigation. The haplotype analysis was conducted using 59 tetraploid wheat accessions (Table S1).

DPW, TPW and their F_1 plants and F_2 population were grown at the Wenjiang experimental field of Sichuan Agricultural University, Chengdu, China, in the 2011–2012 (from October 2011 to June 2012) and 2012–2013 (from October 2012 to June 2013) wheat growing seasons. The F_7 and F_8 RIL populations of DPW×TPW were grown at two experimental fields (Wenjiang and Chongzhou) of Sichuan Agricultural University (Chengdu, China) in the 2017–2018 (from October 2017 to June 2018) and 2018–2019 (from October 2018 to June 2019) wheat growing seasons, respectively. The F_6 RIL population, the F_1 plants of D_60×T_58, two pairs of NILs, and 59 tetraploid wheat accessions were grown at the Wenjiang experimental field in the 2018–2019 (from October 2018 to June 2019) wheat growing season. The F_2 population of D_60×T_58 was grown at the Wenjiang experimental field in the 2019–2020 (from October 2019 to June 2020) wheat growing season. Each line was planted with 20 plants per row. The rows were 2 m long and the spacing between rows was 30 cm.

Phenotypic measurements and analysis

Plant height, spike length, and stem length were measured at maturity. We selected three individual plants per line and calculated the average value. Data was analysed using SPSS software (version 18.0; SPSS, Chicago, IL, USA) Figures were drawn using SigmaPlot software (version 12.0; Systat, Point Richmond, CA, USA).

Homologous cloning of *Rht-B1*

According to the genomic sequence of *T. aestivum* cv. 'Chinese Spring' (IWGSC RefSeq v1.0), a pair of *Rht-B1*-specific primers (forward: 5'-CGATGCCGTC TACAACTACT-3'; reverse: 5'-CAACTCCTAGATCGGGAAACTT-3') was designed using Beacon designer software (version 7.0; Premier Biosoft International, Palo Alto, CA, USA). These primers were used to amplify the full-length Rht-B1 sequence from DPW and TPW. Each PCR reaction mixture contained 2 μl DNA, 2 μl mixture of forward and reverse primers (4 pmol/μl), 2 μl dNTP (2.5 mM/μl), 1 μl Ex-Taq polymerase (5 U/μl), 2 μl $MgCl_2$ (2.5 mM/μl), 2.5 μl 10× PCR buffer, and 13.5 μl ddH_2O. The PCR amplification conditions were 95°C for 5 min, 40 cycles (95°C for 30 s, 58°C for 30 s, and 72°C for 2 min), and final extension at 72°C for 10 min. Each amplified fragment was cloned into the pMD19-T vector for sequencing. Differences in *Rht-B1* sequences between DPW and TPW were detected in an alignment analysis using Vector NTI software (version 11.5.1; Invitrogen, Carlsbad, CA, USA).

Exploitation of indel marker of *Rht-B1* for mapping

According to the sequence differences in *Rht-B1* between DPW and TPW, a pair of *Rht-B1*-specific primers (*Rht-B1 Indel*-F: 5'-GGCGGGAGATCGAAGTAC-3', *Rht-B1 Indel*-R: 5'-GACACCGTGCACTACAAC-3') was designed using Beacon designer software.

Exploitation of SSR markers on 4BS for mapping

According to the genomic sequence of 4BS of *T. aestivum* cv. 'Chinese Spring' (IWGSC RefSeq v1.0) (http://plants.ensembl.org/), microsatellites were predicted using the MIcroSAtellite identification tool (https://webblast.ipk-gatersleben.de/misa/) [31-32]. Beacon designer software was used to design SSR markers (Table S2).

Genotyping and genetic mapping

Genomic DNA was extracted from DPW, TPW, Ailanmai and the mapping populations RIL_6 (DPW×Ailanmai), RIL_7 and RIL_8 (DPW×TPW) using a plant genomic DNA kit (TIANGEN BIOTECH, Beijing, China). Each PCR reaction mixture contained 1 μl DNA, 2 μl mixture of forward and reverse primers (4 pmol/μl), 1.5 μl dNTP (2.5 mM/μl), 0.5 μl Taq polymerase (5 U/μl), 1.5 μl $MgCl_2$ (2.5 mM/μl), 2 μl 10× PCR buffer, and 11.5 μl ddH_2O. The PCR amplification conditions were 95 °C for 5 min, 35 cycles (95°C for 45 s, 58°C for 45 s, and 72°C for 45s), and final extension at 72°C for 7 min. The PCR products were separated on 8% polyacrylamide gels. The polymorphic bands between the parents were used to genotype individual lines of the mapping populations.

The *Rht-B1 Indel* marker and 15 polymorphic SSR markers were first used for genetic mapping of *Rht-dp* in the F_7 RIL population. Then, *Rht-B1Indel* and its four flanking SSR markers (*Xgpw2994.1*, *Xgpw3128.1*, *Xgpw3427.1*, and *Xgpw4800.1*) were further used to confirm the candidate region in the F_8 RIL and F_6 RIL populations. The F_7 RIL population was hybridized on the wheat 55K SNP array by CapitalBio Technology (Beijing, China) (unpublished data).

Linkage analysis was performed using the JoinMap software (version 4.0; Kyazma BV, Wageningen, Netherlands) with a logarithm of odds (LOD) threshold of 3.0. The Kosambi mapping function was used to convert the recombination frequencies into genetic distances (cM) [33].

Haplotype analysis of Rht-B1 in 59 tetraploid wheat accessions

Genomic DNA was extracted from each tetraploid wheat accession using a plant genomic DNA kit (TIANGEN BIOTECH, Beijing, China), and PCR amplification was performed as described in the section "Homologous cloning of *Rht-B1*". The amino acid sequence was deduced using ExPASy software (http://web.expasy.org/ translate/). All sequences were aligned using Vector NTI software (Invitrogen). A phylogenetic tree was constructed using the neighbour-joining algorithm in MEGA5 (https://www.megasoftware.net/).

Expression analysis of *Rht-B1b*

Tissues at the three growth stages (jointing, booting, and grain filling stages) were collected, including roots, basal stems, leaf sheaths, leaf blades, young leaves, lower leaf blades, first and second internodes, flag leafs, and spikes. The collected tissues were snap-frozen in liquid nitrogen and stored at −80 °C until RNA extraction. Total RNA was extracted using a Plant RNA Kit (Omega Bio-Tek, American). cDNA was synthesized using the M-MLV First Strand cDNA Synthesis kit (Invitrogen).

Quantitative real-time PCR (qPCR) was performed on the CFX-96 system as described by Wang et al. using a pair of *Rht-B1b*-specific primers (forward: 5'-GGCGGGAGATCGAAGTAC-3'; reverse: 5'-GACACCGTGCACTACAAC-3') [34]. To normalize gene expression levels, the *Actin* gene was used as the reference gene [34]. Relative expression levels were calculated according to the $2^{\Delta\Delta Ct}$ method using the CFX Manager (version 3.1; Bio-Rad, Hercules, CA, USA).

Transcript analysis of two pairs of NILs

Sample collection

At the booting stage, the first internode was collected individually from two pairs of NILs, and then snap-frozen in liquid nitrogen and stored at −80 °C until RNA extraction.

RNA extraction, library preparation and sequencing

Total RNA was isolated as described above, and RNA degradation and contamination were monitored on 1% agarose gels. A NanoPhotometer® spectrophotometer (Implen GmbH, Munich, Germany) RNA purity was used to check RNA purity. The mRNA was purified from total RNA using poly-T oligo-attached magnetic beads and divided into short fragments using NEBNext First Strand Synthesis Reaction Buffer (5×) (New England Biolabs, Ipswich, MA, USA). The cDNA was synthesized using the fragments as templates and then purified and resolved with EB buffer for the end-repair step and addition of a single adenine (A) nucleotide. To select cDNA fragments 250~300 bp in length, the library fragments were purified with the AMPure XP system (Beckman Coulter, Beverly, CA, USA), and suitable fragments were chosen for a PCR amplification. The PCR products were purified (AMPure XP system) and the library quality was assessed using the Agilent Bioanalyzer 2100 system. The prepared libraries were sequenced on the Illumina Hiseq platform.

RNA-seq data analysis

Raw data (raw reads) of in fastq format were first processed using in-house perl scripts. In this step, clean data (clean reads) were obtained by removing reads containing adapters, reads containing poly-N, and low-quality reads from the raw data. All the downstream analyses were conducted using clean, high-quality data.

The Chinese Spring (IWGSC RefSeq v1.0) reference genome and gene model annotation files were downloaded from the genome website (https://urgi.versailles.inra.fr/download/iwgsc/IWGSC_RefSeq_Assemblies/v1.0). The D genome sequences were excluded

from the reference before mapping the processed reads of the tetraploid lines (A and B genomes). An index of the Chinese Spring reference genome was built using Bowtie v2.2.3 and paired-end clean reads were aligned to the reference genome using TopHat v2.0.12. HTSeq v0.6.1 was used to count the number of reads mapped to each gene. The mean fragments per kilobase of transcript per million mapped reads (FPKM) value for each gene was calculated based on the length of the gene and the number of reads mapped to it [35].

Differential expression analysis

Read counts were adjusted by the edgeR program package through one scaling normalized factor. Analysis of differential gene expression between two pairs of NILs (D33/T35 and D60/T58) was performed using the DEGSeq R package. The *P* values were adjusted using the Benjamini and Hochberg method. A corrected *P*-value of 0.005 and log2 (fold change) of 1 were set as the thresholds for significantly different gene expression.

QPCR for validation

Two differentially expressed genes Auxin-repressed protein (ARP) and *L-ascorbate oxidase homolog* (*ASCO*) from RNA-Seq were verified by qPCR, and their gene-specific primers sequences were *APR* (forward: 5'-ATTAAGCAGTCGCCG TCGAT-3'; reverse: 5'-TCGCTGTAAAGCCAG TCGTA -3') and *ASCO* (forward: 5'-AATGGCAATAGGTTCACAGTAGA-3'; reverse: 5'-CTTCACGAGGAACGAGT AGG-3'), respectively.

Results

Phenotype of plants harbouring *Rht-dp*

The average heights of DPW and TPW were 91.52 ± 2.97 cm and 189.88 ± 1.72 cm, respectively. No significant difference in plant heights between F_1 plants (179.12 ± 3.65 cm) and TPW was observed (Fig. S1). The plant heights of F_2 plants ranged from 65 to 185 cm. According to the frequency distribution of plant height, F_2 plants were separated into two groups of dwarf and tall phenotypes at 110 cm (Fig. 1A). The dwarf and tall phenotype groups included 107 and 294 plants, respectively, consistent with the expected Mendelian segregation ratio of 1:3 ($X^2 = 0.606$, $p < 0.05$). These results validate that *Rht-dp* should be a major recessive gene. However, the separated threshold of plant height with 110 cm was significantly larger than the plant height of DPW with 91.52 ± 2.97 cm, which implied that the effect of *Rht-dp* on reducing plant height might be partially covered by one or more non-allelic loci.

To fine-map *Rht-dp*, two RIL populations including 330 F_7 and 300 F_8 plants were constructed. The plant heights of F_7 and F_8 plants ranged from 65 to 165 cm (Fig. 1B) and from 65 to 170 cm (Fig. 1C), respectively. For the F_7 population, the average heights of dwarf and tall phenotypes were 84.07 ± 1.97 cm and 133.75 ± 2.01 cm, respectively. Compared with the tall phenotype, the lines harbouring *Rht-dp* showed a reduction in plant height of up to 37.14%. The reduced plant height was because of the shortened first internode (by 14.83%), second internode (by 7.15%), and basal internode (by 1.46%), but

the length of the spike was not affected (Fig. 1D). These results indicate that *Rht-dp* reduces plant height mainly by restricting elongation of the first and second internodes at the booting stage.

To validate the candidate region of *Rht-dp* in a different genetic background, an F_6 RIL population including 194 lines derived from DPW×Ailanmai was constructed. The average height of Ailanmai was 100.98 ± 0.37 cm. Ailanmai has a recessive dwarfing gene *Rht22*, which has an additive effect with *Rht-dp*. The RIL population was grouped into dwarf and tall phenotypes with heights ranging from 20 to 60 cm and from 120 to 160 cm, respectively (Fig. 1E).

Characterization of *Rht-dp* in F_1 plants and F_2 population derived from the cross of a pair of NIL

Since genetic analysis suggested that the effect of *Rht-dp* on reducing plant height was probably influenced by one or more non-allelic loci derived from TPW, a QTL analysis was performed on the F_7 RIL population using the wheat 55K SNP array. Beside of a major-locus on 4BS (*Rht-dp*) derived from DPW caused dwarfism, a micro-locus on 5A derived from TPW heightened plant was detected (unpublished data). To further confirm the information of *Rht-dp*, we measured the plant height of F_1 plants and F_2 population derived from the cross of a pair of NIL (D_60 and T_58). The average heights of D_60 and T_58 were 93.52 ± 1.83 cm and 159.67 ± 2.72 cm, respectively; the average plant height of F_1 was 123.23 ± 2.55 cm. Compared with T_58, F_1 plants harbouring *Rht-dp* showed a reduction in plant height up to 22.82%. The plant heights of F_2 plants ranged from 65 to 155 cm. According to the frequency distribution of plant height, F_2 plants were separated into two groups of dwarf and tall phenotypes at 95 cm (Fig. 2). The dwarf and tall phenotype groups included 62 and 182 lines, respectively, consistent with the expected Mendelian segregation ratio of 1:3 ($X^2 = 0.021$, $p < 0.05$). Meanwhile, the separated threshold of plant height with 95 cm was similar to the plant height of D_60 with 93.52 ± 1.83 cm. These results indicate that the dwarfing gene of *Rht-dp* should be a single semi-dominant gene, and further imply that the candidate gene is *Rht-B1b*.

Differences in sequence of *Rht-B1* between DPW and TPW

To test the implication that the candidate gene of *Rht-dp* is *Rht-B1b* or one of its alleles, the sequences of *Rht-B1* were cloned from DPW and TPW. Sequence analysis showed that *Rht-B1* of DPW is *Rht-B1b*, with a single nucleotide change from C to T at the nucleotide position 190 when compared with *Rht-B1a* (Fig. 3A) that results in a premature termination codon at amino acid position 64 (Fig. 3B). Although *Rht-B1* of TPW did not have this single nucleotide change from C to T at nucleotide position 190, it had a three-nucleotide deletion at nucleotide position 386–388 when compared with *Rht-B1a* (Fig. 3A), resulting in a serine (S) deletion at amino acid position 129 (Fig. 3B). These results imply that the candidate gene of *Rht-dp* might be *Rht-B1b*. An *Rht-B1 Indel* marker was developed from the three-nucleotide deletion of *Rht-B1* in TPW for further analysis.

Mapping of *Rht-dp*

To confirm that the candidate gene of *Rht-dp* is *Rht-B1b*, the *Rht-B1Indel* marker was first used to determine whether *Rht-B1* was tightly linked with *Rht-dp*. Genetic mapping analyses confirmed that the *Rht-B1Indel* marker completely co-segregated with *Rht-dp* in three RIL populations and a F_2 population derived from a pair of NIL (Fig. 4).

To further confirm that *Rht-B1b* is located in the candidate region of *Rht-dp*, 190 pairs of SSR markers were exploited according to the genome reference of 4BS (Table S2). Fifteen pairs of SSR markers exhibited polymorphism between DPW and TPW, and were linked with *Rht-dp* in the F_7 RIL population. Of them, two SSR markers, *Xgpw2994.1* and *Xgpw3128.1*, were tightly linked with *Rht-dp* with a genetic distance of 0.6 cM (Fig. 4A; Table S3). *Xgpw2994.1* and *Xgpw3128.1* were further confirmed as tightly linked markers flanking *Rht-dp* in the F_2 population derived from NIL (Fig. 4B), and the F_6 (Fig. 4C) and F_8 (Fig. 4D) RIL populations (Table S3).

Based on the gene annotation of wheat 4BS from 29.94 to 31.29 Mbp, flanked by *Xgpw2994.1* and *Xgpw3128.1*, there were five potential genes: *TraesCS4B01G042700* (encodes a teosinte branched 1 protein), *TraesCS4B01G042800* (encodes an uncharacterized protein), *TraesCS4B01G042900* (a RING finger protein), *TraesCS4B01G043000* (EamA-like transporter family), and *TraesCS4B01G043100* (*Rht-B1* encodes a DELLA protein) (Fig. 4E). Apart from *Rht-B1*, sequence difference of other four genes (primers listed in Table S4) between DPW and TPW was not found. These results indicate that the candidate gene of *Rht-dp* should be *Rht-B1b*.

Expression patterns of *Rht-B1b* in DPW

To confirm that *Rht-B1b* reduces plant height via its effects on elongation of the first and second internodes at the booting stage, the transcriptional patterns of *Rht-B1b* were investigated in different DPW tissues at the jointing, booting, and grain-filling stages. *Rht-B1b* was mainly expressed in the first and second internodes at the booting stage, and at dramatically higher levels in those tissues than in other tissues at the jointing, booting, and grain-filling stages (Fig. 5).

Allelic variations of Rht-B1 in tetraploid wheat accessions

Rht-B1b has never been found in spontaneous tetrapolid accession. Since *Rht-B1b* is the candidate gene of *Rht-dp* in DPW, the haplotypes of *Rht-B1b* in 59 tetraploid wheat accessions were analysed. Among them, five accessions were dwarf phenotypes including two *T. turgidum* (AS313 and AS2239), two *T. polonicum* [AS304 (DPW) and IC12196], and one *T. durum* (ZH2237). The 59 sequences cloned from the 59 tetraploid wheat accessions were grouped into eight types. *Rht-B1b* was only obtained from two *T. polonicum* (DPW and IC12196) accessions; and *Rht-B1t* and *Rht-B1u* were only obtained from *T. turgidum. subsp. dicoccon* (PI191781) and *T. turgidum. subsp. Turanicum* (PI184543), respectively. Of them, five novel types (named *Rht-B1q–B1u*, respectively) were identified by comparison with *Rht-B1a* (Fig. 6B). Rht-B1q contained an S deletion at position 129 (S129); Rht-B1r carried a mutation at position 30 (A30S) and an S deletion at position 129 (S129); Rht-B1s contained a mutation at position 363

(P363S). Rht-B1t had two mutations at positions 15 (G15R) and 363 (P363S). Rht-B1u also had two mutations at positions 136 (Y136D) and 363 (P363S) (Fig. 6B).

Among these variations, Rht-B1q had the highest frequency (43.9%). The frequencies of Rht-B1a, Rht-B1b, Rht-B1h, Rht-B1r, Rht-B1s, Rht-B1t, and Rht-B1u were 15.3%, 3.4%, 13.6%, 13.6%, 6.8%, 1.7%, and 1.7%, respectively.

Dwarfism-related DEGs induced by DELLA mutant Rht-B1b

To understand the molecular networks of *Rht-B1b*, the DEGs induced by the DELLA mutation *Rht-B1b* in the first internode of two pairs of NILs were investigated. A total of 41 DEGs was obtained, 30 of which were successfully functionally annotated (Table S5). Twenty-eight DEGs were further classed into five sub-groups; hormone-related signalling transduction genes, transcription factor genes, cell wall structure-related genes, reactive oxygen-related genes, and nitrogen regulation-related genes (Table 1). Among the hormone-related signal transduction genes, two brassinolide (BR) signal-related genes *serine carboxypeptidase II-3* (*SCP*) and *cytochrome P450 710A1* (*CYP450*) were down-regulated; and genes encoding salicylic acid (SA)-binding protein 2 and ARP were up-regulated in the dwarf phenotype. The only down-regulated transcription factor gene was *MybAS2*. Fifteen DEGs were grouped into cell wall structure-related genes (seven pectin-related genes and eight xylan acetylation-related genes). In the dwarf phenotype, five pectin-related genes [encoding a pectate lyase 15 (PEL15), three subtilisin-like protease (SBT1.7), and an alpha-galactosidase (α-Gal)] involved in pectin modification were down-regulated; while all eight xylan acetylation-related genes, including three *GDSL esterase/lipase* genes, two *ESKIMO* genes, *IRX15-L*, *ALTERED XYLOGLUCAN 4-like* (*AXY-L*), and an uncharacterized acetyltransferase gene were up-regulated. For the reactive oxygen-related genes, *plant cysteine oxidase 2* (*PCO2*) and *ASCO* were down-regulated; and genes encoding germin-like protein 5-1 (GLP) and blue copper protein (BCP) were up-regulated in the dwarf phenotype. For nitrogen assimilation-related genes, two *phosphoenolpyruvate carboxylase kinase 2* (*PPCK2*) genes and *early nodulin* (*ENOD*) were down-regulated; and *asparagine synthetase* (*APS*) was up-regulated in the dwarf phenotype. We verified the expression of *ARP* and *ASCO* in the first and second internodes at the booting stage (Fig. S2).

Discussion

The GA-insensitive dwarfing gene *Rht-B1b* is the predominant source of the semi-dwarf growth habit of wheat plants grown in parts of Northern Europe [36], the Mid and Lower Yangtze Valley Autumn-sown Spring Wheat Region in China [37], and the Great Plains Hard Winter Wheat Region in the USA [38]. Because *Rht-B1b* significantly decreases plant height to reduce plant lodging and increase wheat yield [37, 39], it has been introduced into tetraploid wheat *T. durum* for dwarf breeding [28]. However, it is well known that the progenitor of *T. polonicum* is not Norin 10 or *T. durum*. Additionally, DPW was originally collected from Tulufan, Xingjiang, China [23]. Thus, the dwarfing gene *Rht-dp* of *T. polonicum* cannot be derived from Norin 10 or *T. durum*. However, our results show that the candidate gene *Rht-dp* of DPW is *Rht-B1b*. This conclusion is supported by the following evidences: (1) *Rht-dp* is a single semi-dominant

dwarfing gene, as is *Rht-B1b* [6]. (2) *Rht-dp* and *Rht-B1b* reduce plant height mainly via reducing the length of the first and second internodes (Fig. 1D), and their effects on reducing plant height are similar with 22% [18, 39]. (3) The sequence of *Rht-B1* of DPW is the same as that of *Rht-B1b* (Fig. 3). (4) Mapping work revealed that the candidate region of *Rht-dp* was between SSR markers *Xgpw2994.1* and *Xgpw3128.1* (Fig. 4B-D). This region contains five potential genes including *Rht-B1* (Fig. 4E); except of *Rht-B1*, other four genes have no sequence difference between DPW and TPW. (5) The *Rht-B1 Indel* marker developed based on the sequence difference of *Rht-B1* between DPW and TPW is completely co-segregated with *Rht-dp* in a F_2 population derived from NIL and three RIL populations (Fig. 4). In the haplotype analysis, *Rht-B1b* was only obtained from *T. polonicum* (Fig. 6A), implying that it might originate from this species, or might be introduced into *T. polonicum* from other unknown species but not *T. aethiopicum* and *T. durum*.

In wheat, *Rht-B1b* encodes a DELLA mutant protein resembling the SLRL1 protein. Its accumulation represses GA-regulated growth and developmental responses and causes the typical semi-dwarf phenotype [6, 40]. DELLA not only regulates the expression of downstream genes but also interacts with DNA-binding transcription factors. Our transcript analysis identified 28 DEGs regulated by the DELLA mutant *Rht-B1b* involved in the processes of nitrogen assimilation, oxidation-reduction, modification of the cell wall components and structures, and hormone-related signal transduction (Table 1). However, this list of DEGs only slightly overlaps with those identified in previous studies, suggesting that the effects of DELLA on transcription depend on the species, organ, and developmental context [41-44]. Since *Rht-B1b* is mainly expressed in the first and second internodes (Fig. 5) to dramatically reduce their lengths at the booting stage in DPW (Fig. 1D), we explored the molecular network of *Rht-dp* by conducting a transcript analysis of the first and second internodes at the booting stage.

The control of plant growth and development by DELLA is dependent on GA-regulated growth and developmental responses [44-46]. However, we did not find genes involved in GA metabolism among the DEGs in this study. Instead, the DEGs identified in this study included auxin-, SA- and BR-related genes (Table 1). These results suggested that GA interacts with these hormones [46]. DELLA can directly trigger the expression of auxin- and BR-related genes to affect plant growth [47-48]. For example, the expressions of *SCP* and *CYP450* (both grouped into BR-related genes) were dramatically down-regulated by the DELLA mutation *Rht-B1b* to potentially cause dwarfism in DPW (Table 1), because the expression of *SCP* positively affects plant growth [49]. Auxin represses the expression of *ARP* genes [50-51]. In a previous study, overexpression of an *ARP* of *Brassica rapa* caused a reduction in vegetative growth [50]. Auxin also modulates the expression of *ASCO*, which encodes a crucial enzyme that produces oxidative molecules, including H_2O_2 [52]. Overexpression of an *ASCO* in cotton enhanced the accumulation of H_2O_2 and promoted cell elongation, whereas suppression of an *ASCO* in tobacco and *Arabidopsis* inhibited stem cell growth [53]. Our results show that the DELLA mutation *Rht-B1b* resulted in dramatically up-regulated *ARP* and down-regulated *ASCO* in DPW (Table 1). Auxin-induced growth inhibition is accompanied by decreased levels of reactive oxygen species [54]. Thus, the accumulation of the DELLA mutant protein

regulated via auxin-mediated signal transduction may reduce the contents of reactive oxygen species such as H_2O_2 [41], thereby limiting cell expansion to cause dwarfism in DPW.

In rice, over-expression of an *early nodulin* gene resulted in improved nitrogen-use efficiency and increased nitrogen assimilation [55]. In C_3 plants, nitrogen assimilation is positively correlated with phosphoenolpyruvate carboxylase (PEPC) phosphorylation [56-57], which is catalysed by phosphoenolpyruvate carboxylase kinase (PPCK). The extent of phosphorylation is largely determined by PPCK activity, which is controlled by the level of *PPCK* transcripts [56, 58-59]. A reduction in PEPC activity leads to serious stunting of growth [60]. Our results showed that the DELLA mutation *Rht-B1b* led to significant down-regulation of *early nodulin* and two *PPCKs* in DPW (Table 1). Thus, decreased nitrogen assimilation and PPCK activity may decrease the activity of PEPC [43, 59] to cause dwarfism in DPW.

The hemicellulose xylan and pectins are two abundant polysaccharides in the plant cell wall [61]. Their modifications, such as methylesterification and acetylation, have been proposed to influence cell wall architecture and function, causing various plant growth phenotypes [61-64]. Our results showed that the DELLA mutation *Rht-B1b* led to significant down-regulation of the expression of several pectin-related genes, including *PEL*, three *SBTs,* and *α-Gal* (Table 1). Decreases in the transcript levels of these genes may lead to the repression of pectin degradation and the accumulation of de-esterified pectin [63], enhanced pectin methylesterase activity to stiffen the cell wall [65], and reduced adherence of pectin to the cell wall [66]. Thus, the DELLA mutation *Rht-B1b* may result in modifications of pectin that limit cell wall loosening and inhibit cell elongation, thereby causing dwarfism in DPW.

Many studies have reported that either excess or inadequate acetylation of xylan disrupts the cell wall structure, thereby causing dwarfism in plants. Our results show that the DELLA mutation *Rht-B1b* up-regulated eight xylan acetylation-related genes, including three *GDSL esterase/lipase* genes, two *ESKIMO* genes, *IRX15-L*, *AXY-L,* and an uncharacterized acetyltransferase gene (Table 1). ESKIMO and AXY-L are xylan acetyltransferases, and IRX-L is involved in synthesis of the xylan backbone [61, 69-70]. A specific interaction between acetyltransferases and xylan backbone biosynthetic enzymes may repress acetylation of adjacent residues [70]. Therefore, even though the transcript levels of *ESKIMO*, *IRX15-L*, *AXY-L* and IRX-L were up-regulated (Table 1), the acetylation of xylan might be decreased. GDSL esterase/lipase is a xylan deacetylation enzyme [64]. The DELLA mutation *Rht-B1b* resulted in up-regulated expression of *GDSL esterase/lipase*, leading to enhance xylan deacetylation. Therefore, the DELLA mutation *Rht-B1b* may reduce acetylation of xylan to limit cell wall loosening and inhibit cell elongation, causing dwarfism in DPW.

A model summarizing how the DELLA mutation *Rht-dp* causes dwarfism in DPW is proposed (Fig. 7). Whether the DELLA mutation *Rht-B1b* regulates the pathway of hormones, reactive oxygen species, and nitrogen assimilation, it ultimately affects the cell wall structure to limit cell wall loosening and inhibit cell elongation, thereby causing dwarfism in DPW.

Conclusion

In summary, our results indicated that the semi-dwarfing gene *Rht-dp* is the“Green Revolution” gene *Rht-B1b*. It regulates pathways related to hormones, reactive oxygen species, and nitrogen assimilation to modify the cell wall structure, and then limits cell wall loosening and inhibits cell elongation, thereby causing dwarfism in DPW.

Abbreviations

BR, brassinolide; cM, centimorgan; DEGs, differentially expressed genes; DPW, dwarf polish wheat; FPKM, fragments per kilobase of transcript per million mapped reads; GA, gibberellin; Jianyangailanmai, Ailanmai; LOD, logarithm of odds; NIL, near-isogenic line; qPCR, Quantitative real-time PCR; RIL, recombinant inbred line; RNA-seq, RNA sequencing; SA, salicylic acid; TPW, tall polish wheat.

Declarations

Ethics approval and consent to participate

The DPW and TPW lines were originally collected from Tulufan, Xinjiang province, China, by Prof. Chi Yen and Junliang Yang (Sichuan Agricultural University, China) in the 1980s. No permission was necessary to collect this sample. Professor Chi Yen undertook the formal identification of the sample. The voucher specimen and the seed are deposited in the Triticeae Research Institute, Sichuan Agricultural University, Chengdu, Sichuan, China. Collection of the dwarf Polish wheat complied with the institutional, national and international guidelines.

Consent for publication

Not applicable.

Availability of data and materials

All data generated or analyzed during this study were included in this article and the supplementary files.

Funding

This work was supported by the National Natural Science Foundation of China (No 31671688), and the Bureau of Science and Technology of Sichuan Province, China.

Competing interest

The authors declare that they have no conflicts of interest.

Authors’ contributions

SC, XX, JL, YW and YZ designed the research and wrote the manuscript; SC, QY, XZ and XX performed the experiments; SC, XF, JZ, LS, HK, HZ and YW performed the data analysis and revised the manuscript.

Acknowledgements

We thank the professor Lianquan Zhang (Sichuan Agricultural University, China) who provided the grain of tetraploid wheat accessions for haplotype analysis.

References

1. Gale MD, Youssefian S, Russell GE. Dwarfing genes in wheat. Progress in Plant Breeding 1985;1-35.
2. Flintham JE, Börner A, Worland AJ, Gale MD. Optimizing wheat grain yield: effects of *Rht* (gibberellin-insensitive) dwarfing genes. J Agri Sci 1997; 128(1):11-25.
3. Youssefian S, Kirby EJM, Gale MD. Pleiotropic effects of the GA- insensitive *Rht* dwarfing genes in wheat. 2. Effects on leaf, stem, ear and floret growth. Field Crop Res. 1992;28(3):191-210.
4. Hedden P. The genes of the Green Revolution. Trends Genet. 2003;19(1):5-9.
5. Hong Z, Ueguchi-Tanaka M, Shimizu-Sato S, Inukai Y, Fujioka S. Loss- of-function of a rice brassinosteroid biosynthetic enzyme, C-6 oxidase, prevents the organized arrangement and polar elongation of cells in the leaves and stem. Plant J. 2002;32(4):495-508.
6. Peng JR, Richards DE, Hartley NM, Murphy GP, Devos KM, Flintham JE, Beales J, Fish LJ, Worland AJ, Pelica F, Sudhakar D, Christou P, Snape JW, Gale MD, Harberd NP. 'Green Revolution' genes encode mutant gibberellin response modulators. 1999;400(6741):256.
7. Sasaki A, AshikariM, Ueguchi-Tanaka M, Itoh H, Nishimura A, Swapan D, Ishiyama K, Saito T, Kobayashi M, Khush GS, Kitano H, Matsuoka M. Green revolution: A mutant gibberellin- synthesis gene in rice. 2002;416(6882):701-702.
8. Chen SL, Gao RH, Wang HY, Wen MX, Xiao J, Bian NF, Zhang RQ, Hu WJ, Cheng SH, Bie TD, Wang XU. Characterization of a novel reduced height gene (*Rht23*) regulating panicle morphology and plant architecture in bread wheat. 2015;203(3):583-594.
9. Ellis MH, Rebetzke GJ, Azanza F, Richards RA, Spielmeyer W. Molecular mapping of gibberellin-responsive dwarfing genes in bread wheat. Appl. Genet. 2005;111(3):423-430.
10. Kang HY, Lin LJ, Song ZJ, Yuan JY, Zhong MY, Zhang HQ, Fan X, Sha LN, Wang Y, Xu LL, Zeng J, Zhou YH. Identification, fine mapping and characterization of *Rht-dp*, a recessive wheat dwarfing (reduced height) gene derived from *Triticum polonicum*. Genes Genom. 2012;34(5):509-515.
11. Mo Y, Vanzetti LS, Hale I, Spagnolo EJ, Guidobaldi F, Al-Oboudi J, Dubcovsky Identification and characterization of *Rht25*, a locus on chromosome arm 6AS affecting wheat plant height, heading time, and spike development. Theor Appl Genet. 2018;131(10):2021-2035.
12. Pearce S, Saville R, Vaughan SP, Chandler PM, Wilhelm EP, Sparks CA, Hedden P. Molecular characterization of *Rht-1* dwarfing genes in hexaploid wheat. Plant Physiol. 2011;157(4):1820-1831.
13. Vikhe P, Patil RM, Chavan A, Oak MD, Tamhankar SA. Mapping gibberellin- sensitive dwarfing locus *Rht18* in durum wheat and development of SSR and SNP markers for selection in breeding. Mol Breeding. 2017;37(3):28.

14. Watanabe Triticum polonicum IC^{12196}: a possible alternative source of GA3-insensitive semi-dwarfism. Cereal Res Commun. 2004;32(4) 429-434.
15. Watanabe N. Genetic mapping of the genes and development of near-isogenic lines in durum wheat. EWAC Newsletters. 2008;27-28.
16. Würschum T, Langer SM, Longin CFH, Tucker MR, Leiser WL. A modern green revolution gene for reduced height in wheat. Plant J. 2017;92(5):892-903.
17. Gasperini D, Greenland A, Hedden P, Dreos R, Harwood W, Griffiths S. Genetic and physiological analysis of *Rht8* in bread wheat: an alternative source of semi-dwarfism with a reduced sensitivity to brassinosteroids. J Exp Bot. 2012;63(12):6760.
18. Rebetzke GJ, Ellis MH, Bonnett DG, Mickelson B, Condon AG, Richards RA. Height reduction and agronomic performance for selected gibberellin-responsive dwarfing genes in bread wheat (*Triticum aestivum* L). Field Crop Res. 2012;126:87-96.
19. Haque MA, Martinek P, Kobayashi S, Kita I, Ohwaku K, Watanabe N, Kuboyama T. Microsatellite mapping of genes for semi-dwarfism and branched spike in *Triticum durum* Desf var *ramosoobscurum Jakubz* "Vetvistokoloskaya". Genet Resour Crop Ev. 2012;59(5):831-837.
20. Konzak CF. Mutations and mutation breeding. Wisconsin, American: Heyne EG (ed) wheat and wheat improvement 2nd Edition American Society of Agronomy. 1987;428-443.
21. Peng ZS, Li X, Yang ZJ, Liao ML. A new reduced height gene found in the tetraploid semi-dwarf wheat landrace Aiganfanmai. Genet Mol Res. 2011;10(4):2349-2357.
22. Wiwart M, Suchowilska E, Kandler W, Sulyok M, Groenwald P, Krska R. Can Polish wheat (*Triticum polonicum L*) be an interesting gene source for breeding wheat cultivars with increased resistance to Fusarium head blight. Genet Resour Crop Ev. 2013;60(8):2359-2373.
23. Liu GX, Zhou YH, Zheng YL, Yang RW, Ding CB. The reaction of hormone gibberellic acid in dwarfing polish wheat (*Triticum polonicum*) from Tulufan, Xinjiang. J Sichuan Agric Univ. 2002;20:81-83.
24. Wang Y, Xiao X, Wang XL, Zeng J, Kang HY, Fan X, Sha LN, Zhang HQ, Zhou YH. RNA-Seq and iTRAQ reveal the dwarfing mechanism of dwarf polish wheat (*Triticum polonicum* L). Int J Bio Sci. 2016;12(6):653.
25. Bazhenov MS, Divashuk MG, Amagai Y, Watanabe N, Karlov GI. Isolation of the dwarfing *Rht-B1p* (*Rht17*) gene from wheat and the development of an allele-specific PCR marker. Mol Breeding. 2015;35(11):1-8.
26. Wen W, Deng QY, Jia HY, Wei LZ, Wei JB, Wan HS, Yang LM, Cao WJ, Ma ZQ. Sequence variations of the partially dominant DELLA gene *Rht-B1c* in wheat and their functional impacts. J Exp Bot. 2013;64(11):3299-3312.
27. Reitz LP, Salmon SC. Origin, History, and Use of Norin 10 Wheat 1. Crop Sci. 1968;8:686-689.
28. Quick JS, Miller JD, Donnelly BJ. Cando North Dakota's First Semidwarf Durum. North Dakota Farm Res. 1976;33:15-18.

29. Börner A, Plaschke J, Korzun V, Worland AJ. The relationships between the dwarfing genes of wheat and rye. 1996;89(1):69-75.
30. Haque MA, Martinek P, Watanabe N, Kuboyama T. Genetic mapping of gibberellic acid-sensitive genes for semi-dwarfism in durum wheat. Cereal Res Commun. 2011;39(2):171-178.
31. Beier S, Thiel T, Münch T, Scholz U, Mascher M. MISA-web: a web server for microsatellite prediction. 2017;33(16):2583-2585.
32. Thiel T, Michalek W, Varshney RK, Graner A. Exploiting EST databases for the development and characterization of gene-derived SSR-markers in barley (*Hordeum vulgare L*). Theor Appl Genet. 2003;106(3):411-422.
33. Kosambi DD. The estimation of map distances from recombination values. Ann Hum Genet. 1943;12(1):172-175.
34. Wang Y, Wang XL, Gu MX, Kang HY, Zeng J, Fan X, Sha LN, Yu KF, Zhou YH. Cloning and characterization of four novel *SnRK2* genes from *Triticum polonicum*. Biol Plantarum. 2015;59(2):211-219.
35. Trapnell C, Roberts A, Goff L, Pertea, Kim GD, Kelley DR, Pimentel H, Salzberg SL, Rinn JL, Pachter L. Differential gene and transcript expression analysis of RNA-seq experiments with TopHat and Cufflinks. Nat Protoc. 2012;7(3):562.
36. Knopf C, Becker HC, Ebmeyer E, Korzun V. Occurrence of three dwarfing *Rht* genes in German winter wheat varieties. Cereal Res Commun. 2008;36(4):553- 560.
37. Zhang XK, Yang SJ, Zhou Y, He ZH, Xia XC. Distribution of the *Rht-B1b*, *Rht-D1b* and *Rht8* reduced height genes in autumn-sown Chinese wheats detected by molecular markers. Euphytica. 2006;152(1):109-116.
38. Guedira M, Brown-Guedira G, Van Sanford DA, Sneller C, Souza E, Marshall D. Distribution of *Rht* genes in modern and historic winter wheat cultivars from the eastern and central USA. Crop Sci. 2010;50(5):1811-1822.
39. Liu Y, Zhang J, Hu YG, Chen J. Dwarfing genes *Rht4* and *Rht-B1b* affect plant height and key agronomic traits in common wheat under two water regimes. Field Crop Res. 2017;204(204):242-248.
40. Van De Velde K, Ruelens P, Geuten K, Rohde A, Van Der Straeten D. Exploiting DELLA signaling in cereals. Trends Plant Sci. 2017;22(10):880-893.
41. Achard P, Renou JP, BerthoméR, Harberd NP, Genschik P. Plant DELLAs restrain growth and promote survival of adversity by reducing the levels of reactive oxygen species. Curr Biol. 2008;18(9):656-660.
42. Carrera E, Ruiz-Rivero O, Peres LE, Atares A, Garcia-Martinez JL. Characterization of the procera tomato mutant shows novel functions of the SlDELLA protein in the control flower morphology, cell division and expansion, and the auxin-signaling pathway during fruit-set and development. Plant Physiol. 2012;160(3):1581-1596.
43. Li S, Tian YH, Wu K, Ye YF, Yu JP, Zhang JQ, Liu Q, Hu MY, Li H, Tong YP, Harberd NP, Fu XD. Modulating plant growth–metabolism coordination for sustainable agriculture. 2018;560(7720):595-

600.

44. Locascio A, Blázquez MA, Alabadí D. Genomic analysis of DELLA protein activity. Plant Cell Physiol. 2013;54(8):1229-1237.
45. Cao DN, Cheng H, Wu, W Soo HM, Peng JR. Gibberellin mobilizes distinct DELLA-dependent transcriptomes to regulate seed germination and floral development in Arabidopsis. Plant Physiol. 2006;142(2):509-525.
46. Claeys H, De Bodt S, InzéD. Gibberellins and DELLAs: central nodes in growth regulatory networks. Trends Plant Sci. 2014;19(4):231-239.
47. Bai MY, Shang, JX Oh E, Fan M, Bai Y, Zentella R, Suin TP, Wang ZY. Brassinosteroid gibberellin and phytochrome impinge on a common transcription module in Arabidopsis. Nat Cell Biol. 2012;14(8):810-817.
48. Willige BC, Losno E, Richter R, Zourelidou M, Schwechheimer C. Gibberellin regulates PIN-FORMED abundance and is required for auxin transport-dependent growth and development in *Arabidopsis thaliana*. Plant Cell. 2011;23(6):2184-2195.
49. Zhou AF, Li J. *Arabidopsis BRS1* is a secreted and active serine carboxypeptidase. J Biol Chem. 2005;280(42):35554-35561.
50. Lee J, Han CT, Hur Y. Molecular characterization of the *Brassica rapa* auxin-repressed, superfamily genes, *BrARP1* and *BrDRM1*. Mol Biol Rep. 2013;40(1):197-209.
51. Park S, Han KH. An auxin-repressed gene (*RpARP*) from black locust (*Robinia pseudoacacia*) is posttranscriptionally regulated and negatively associated with shoot elongation. Tree Physiol. 2003;23(12):815-823.
52. Li R, Xin S, Tao CC, Jin X, Li HB. Cotton ascorbate oxidase promotes cell growth in cultured Tobacco Bright Yellow-2 cell through generation of apoplast oxidation. Int J Mol Sci. 2017;18(7):1346.
53. Yamamoto A, Bhuiyan MN, Waditee R, Tanaka Y, Esaka M, Oba K, Jagendorf AT, Takabe T. Supressed expression of the appoplastic *ascorbate oxidase* gene increases salt tolerance in tobacco and *Arabidopsis* J Exp Bot. 2005;56(417):1785-1796.
54. Liszkay A, Der Zalm EV, Schopfer P. Production of reactive oxygen intermediates (O_2^-, H_2O_2 and OH) by maize roots and their role in wall loosening and elongation growth. Plant Physiol. 2004;136(2):3114-3123.
55. Bi YM, Kant S, Clark J, Gidda S, Ming F, Xu JY, Rochon A, Shelp BJ, Hao LX, Zhao R, Mullen RT, Zhu T, Rothstein SJ. Increased nitrogen-use efficiency in transgenic rice plants over-expressing a nitrogen-responsive early nodulin gene identified from rice expression profiling. Plant Cell Environ. 2009;32(12):1749-1760.
56. Fukayama H, Tamai, T Taniguchi Y, Sullivan S, Miyao M, Nimmo HG. Characterization and functional analysis of phosphoenolpyruvate carboxylase kinase genes in rice. Plant J. 2006;47(2):258-268.
57. Van Quy L, Foyper C, Champigny ML. Effect of light and NO_3^- on wheat leaf phosphoenolpyruvate carboxylase activity: evidence for covalent modification of the C_3 Plant Physiol. 1991;97(4):1476-

1482.

58. Chollet R, Vidal J, O'Leary MH. Phosphoenolpyruvate carboxylase: a ubiquitous, highly regulated enzyme in plants, Annual Review of Plant Physiology and Plant. Molecular Biology. 1996;47(1):273-298.
59. Nimmo HG. Control of the phosphorylation of phosphoenolpyruvate carboxylase in higher plants. Arch Bioche Biophysisc. 2003;414(2):189-196.
60. Chen L, Hao L, Condon AG, Hu YG. Exogenous GA3 application can compensate the morphogenetic effects of the GA-responsive dwarfing gene *Rht12* in bread wheat. PloS One. 2014;9(1):e86431.
61. Schultink A, Naylor D, Dama M, Pauly M. The role of the plant-specific ALTERED XYLOGLUCAN19 protein in Arabidopsis cell wall polysaccharide O-acetylation. Plant Physiol. 2015;167(4):1271-1283.
62. Sénéchal F, Graff L, Surcout, O Marcelo P, Rayon C, Bouton S, Mareck A, Mouille G, Stintzi A, Höfte H, Lerouge P, Schaller A, Pelloux J. Arabidopsis *PECTIN METHYLESTERASE17* is co-expressed with and processed by SBT35, a subtilisin-like serine protease. Ann Bot. 2014;114(6):1161-1175.
63. Wang HH, Guo Y, Lv F, Zhu HY, Wu SJ, Jiang YJ, Li FF, Zhou BL, Guo WZ, Zhang TZ, The essential role of *GhPEL* gene, encoding a pectate lyase, in cell wall loosening by depolymerization of the de-esterified pectin during fiber elongation in cotton. Plant Mol Biol. 2010;72(s4-5):397-406.
64. Zhang BC, Zhang LJ, Li F, Zhang DM, Liu XL, Wang H, Xu ZP, Chu CC, Zhou YH. Control of secondary cell wall patterning involves xylan deaceylation by a GDSL esterase. Nat Plants. 2017;3:17017.
65. Schaller A, Stintzi A, Graff L. Subtilases-versatile tools for protein turnover, plant development, and interactions with the environment. Plant Plantarum. 2012;145(1):52-66.
66. Voiniciuc C, Heinrich-Wilhelm Schmidt M, Berger A, Yang B, Ebert B, Scheller HV, North HM, Usadel B, Günl M. MUCILAGE-RELATED10 produces galactoglucomannan that maintains pectin and cellulose architecture in Arabidopsis seed mucilage. Plant Physiol. 2015;169(1):403-420.
67. Lefebvre V, Fortabat MN, Ducamp A, North HM, Maia-Grondard A, Trouverie J, Boursiac Y, Mouille G, Durand-Tardif M. ESKIMO1 disruption in *Arabidopsis* alters vascular tissue and impairs water transport. PloS One. 2011;6(2):e16645.
68. Manabe Y, Verhertbruggen Y, Gille S, Harholt J, Chong SL, Pawar PMA, Mellerowicz EJ, Tenkanen M, Cheng K, Pauly M, Scheller HV. Reduced wall acetylation proteins play vital and distinct roles in cell wall O-acetylaton in *Arabidopsis thaliana*. Plant Physiol. 2013;163(3):1107-1117.
69. Busse-Wicher M, Gomes TCF, Tryfona T, Nikolovski N, Stott K, Grantham NJ, Bolam DN, Skaf MS, Dupree P. The pattern of xylan acetylation suggests xylan may interact with cellulose microfibrils as a twofold helical screw in the secondary plant cell wall of *Arabidopsis thaliana*. Plant J. 2014;79(3):492-506.
70. Jensen JK, Kim H, Cocuron JC, Orler R, Ralph J, Wilkerson CG. The DUF579 domain containing proteins IRX15 and IRX15-L affect xylan synthesis in Arabidopsis. Plant J. 2011;66(3):387-400.

Table

Table 1 Dwarfism-related DEGs induced by DELLA mutant *Rht-dp*

Gene ID	Description	Fold change of transcript	
		D_60/T_58	D_33/T_35
Hormone-related signaling transduction genes			
TraesCS2B01G157100	Serine carboxypeptidase II-3	-32	-20
TraesCS3B01G167400	Cytochrome P450 710A1	-25	-18
TraesCS2B01G471800	Salicylic acid-binding protein 2	28	39
TraesCS4B01G070300	Auxin-repressed 125 kDa protein	12	15
Transcription factor			
TraesCS1B01G055200	Myb-related protein MYBAS2	-13	-26
Cell wall structure-related genes			
Pectin-related genes			
TraesCS2A01G016500	Pectate lyase 15	-17	-29
TraesCS4A01G237500	Subtilisin-like protease SBT17	-20	-22
TraesCS4B01G077600	Subtilisin-like protease SBT17	-29	-17
TraesCS6A01G339400	Subtilisin-like protease SBT17	-14	-12
TraesCS6B01G332900	Alpha-galactosidase	-16	-11
TraesCS1B01G249000	(1-3,1-4)-beta-D-glucanase	21	28
TraesCS2A01G341400	Sugar transport protein 5	11	14
Xylan acetylation-related genes			
TraesCS3A01G258100	GDSL esterase/lipase	15	11
TraesCS3B01G290800	GDSL esterase/lipase	13	10
TraesCS7B01G250700	GDSL esterase/lipase	13	23
TraesCS4A01G110000	ESKIMO 1	14	10
TraesCS4B01G194100	ESKIMO 1	17	10
TraesCS6A01G131900	IRX15-like	13	11
TraesCS7A01G191700	ALTERED XYLOGLUCAN 4-like	17	11
TraesCSU01G204900	Uncharacterized acetyltransferase	28	16
Reactive oxygen-related genes			
TraesCS5A01G025200	Plant cysteine oxidase 2	-11	-15

TraesCS7A01G459400	L-ascorbate oxidase homolog	-34	-51
TraesCS3A01G165500	Germin-like protein 5-1	16	22
TraesCS6A01G315800	Blue copper protein	13	12
Nitrogen regulation-related genes			
TraesCS6A01G375800	Phosphoenolpyruvate carboxylase kinase 2	-12	-20
TraesCS6B01G413500	Phosphoenolpyruvate carboxylase kinase 2	-12	-15
TraesCS7A01G091800	Early nodulin-93	-40	-12
TraesCS3B01G385400	Asparagine synthetase	11	12

Figures

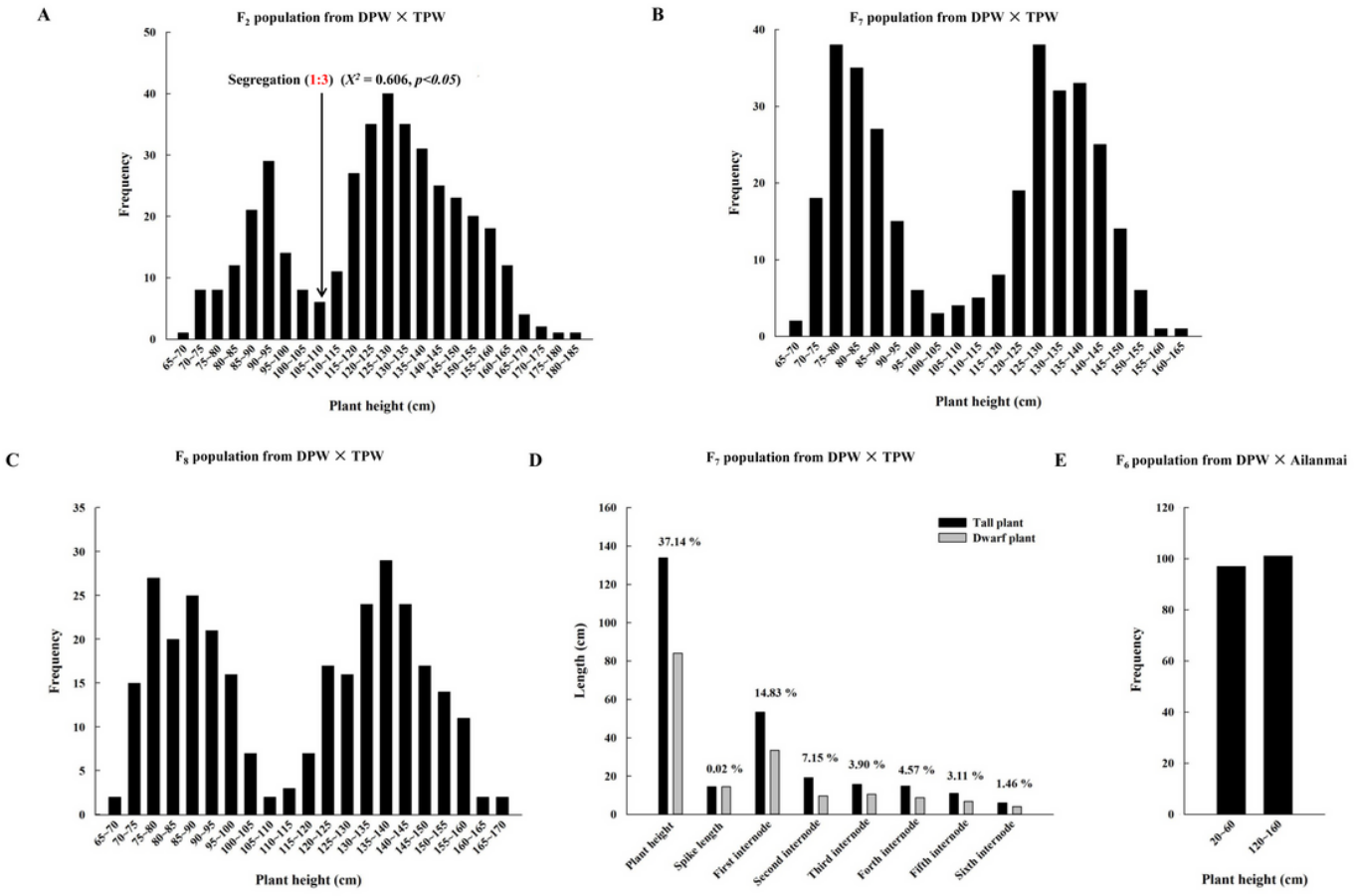


Figure 1

Phenotypic characterization. A: frequency distribution of plant heights in the F2 population from DPW×TPW; B: frequency distribution of plant heights in the DPW×TPW F7 population; C: frequency distribution of plant heights in the DPW×Ailanmai F6 population; D: plant height, the lengths of spike and

each internode of DPW×TPW NILs F7 at the maturate stage; E: frequency distribution of plant heights in the DPW×TPW F8 population.

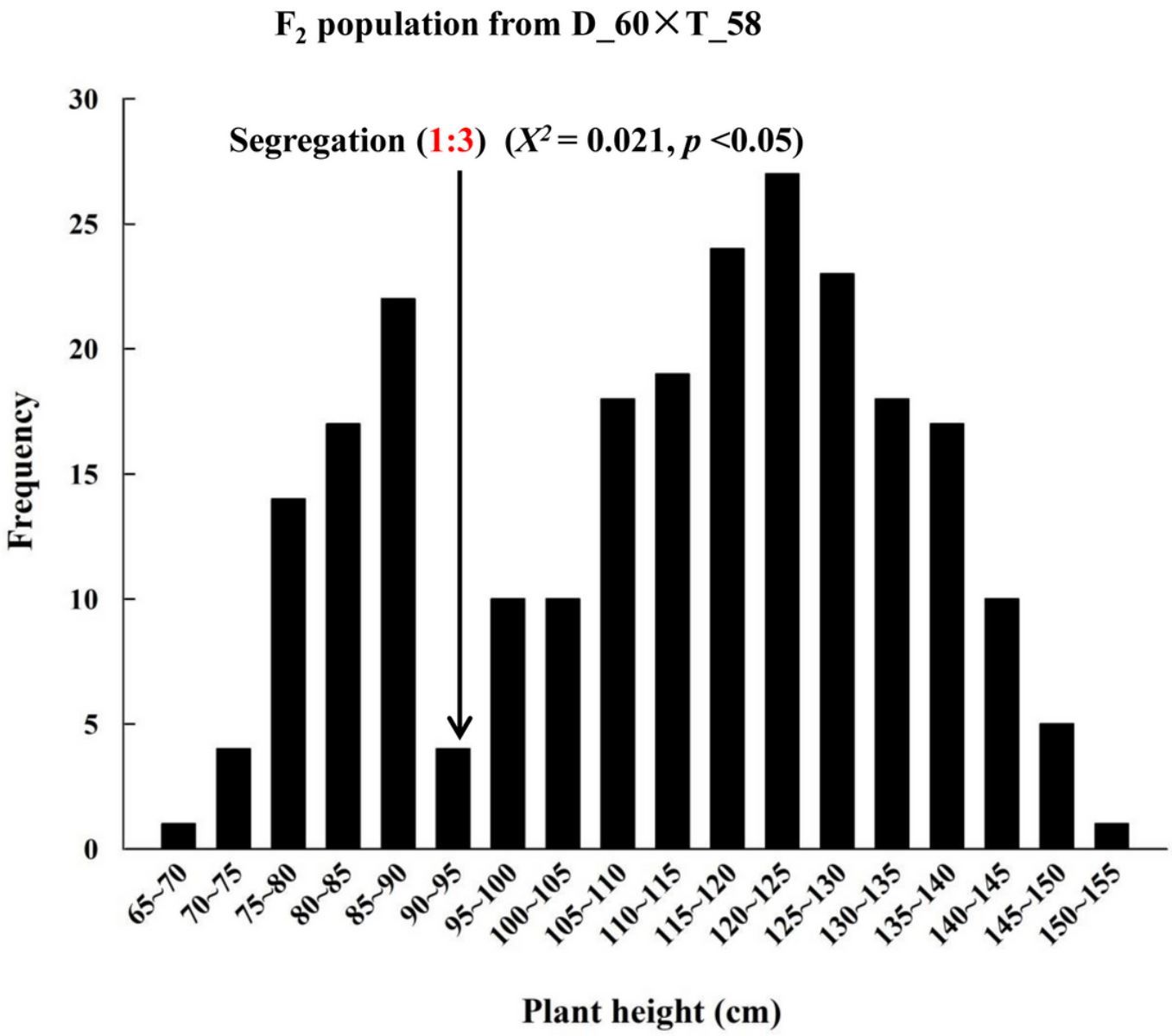


Figure 2

Frequency distribution of plant heights in the F2 population from D_60×T_58.

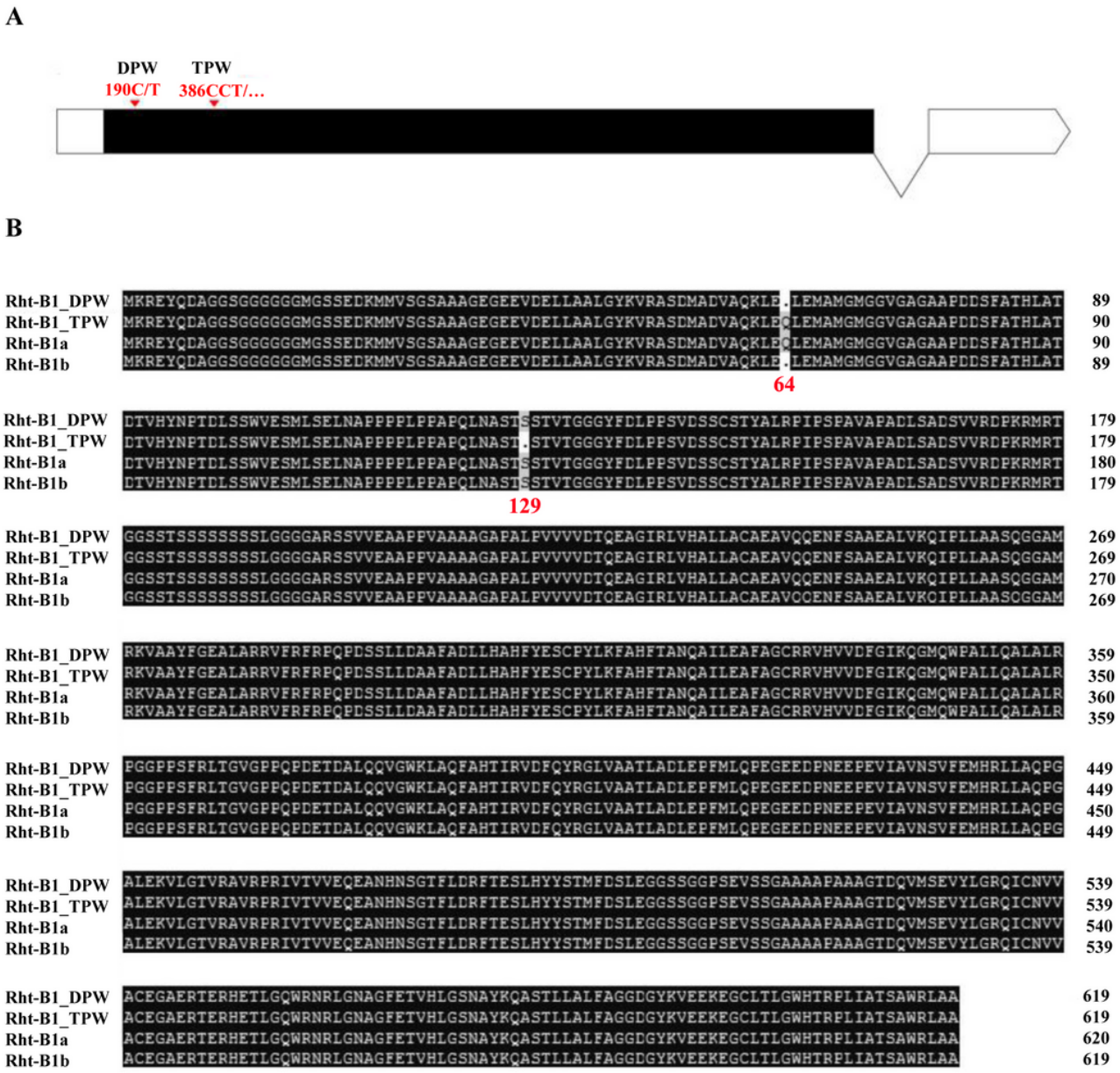


Figure 3

Sequences of Rht-B1 in DPW and TPW. A: nucleotide mutations of Rht-B1 in DPW and TPW; B: amino acid mutations of Rht-B1 in DPW and TPW.

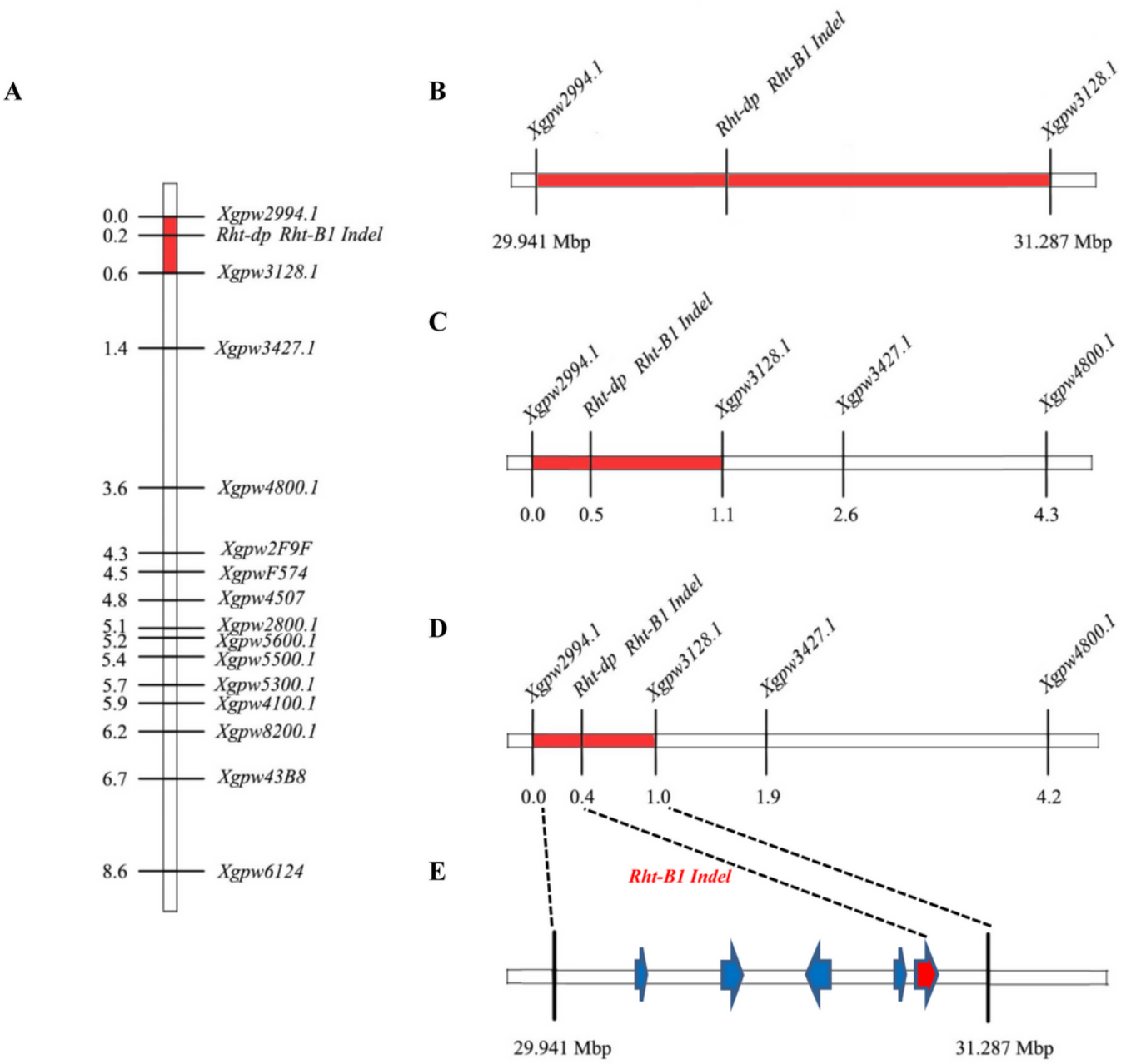


Figure 4

Mapping of Rht-dp. A: mapping of Rht-dp in the DPW×TPW RILs F7; B: mapping of Rht-dp in the F2 population from D_60×T_58; C: mapping of Rht-dp in DPW×Ailanmai RILs F6; D: mapping of Rht-dp in DPW×TPW RILs F8; E: candidate genes between SSR markers Xgpw2994.1 and Xgpw3128.1.

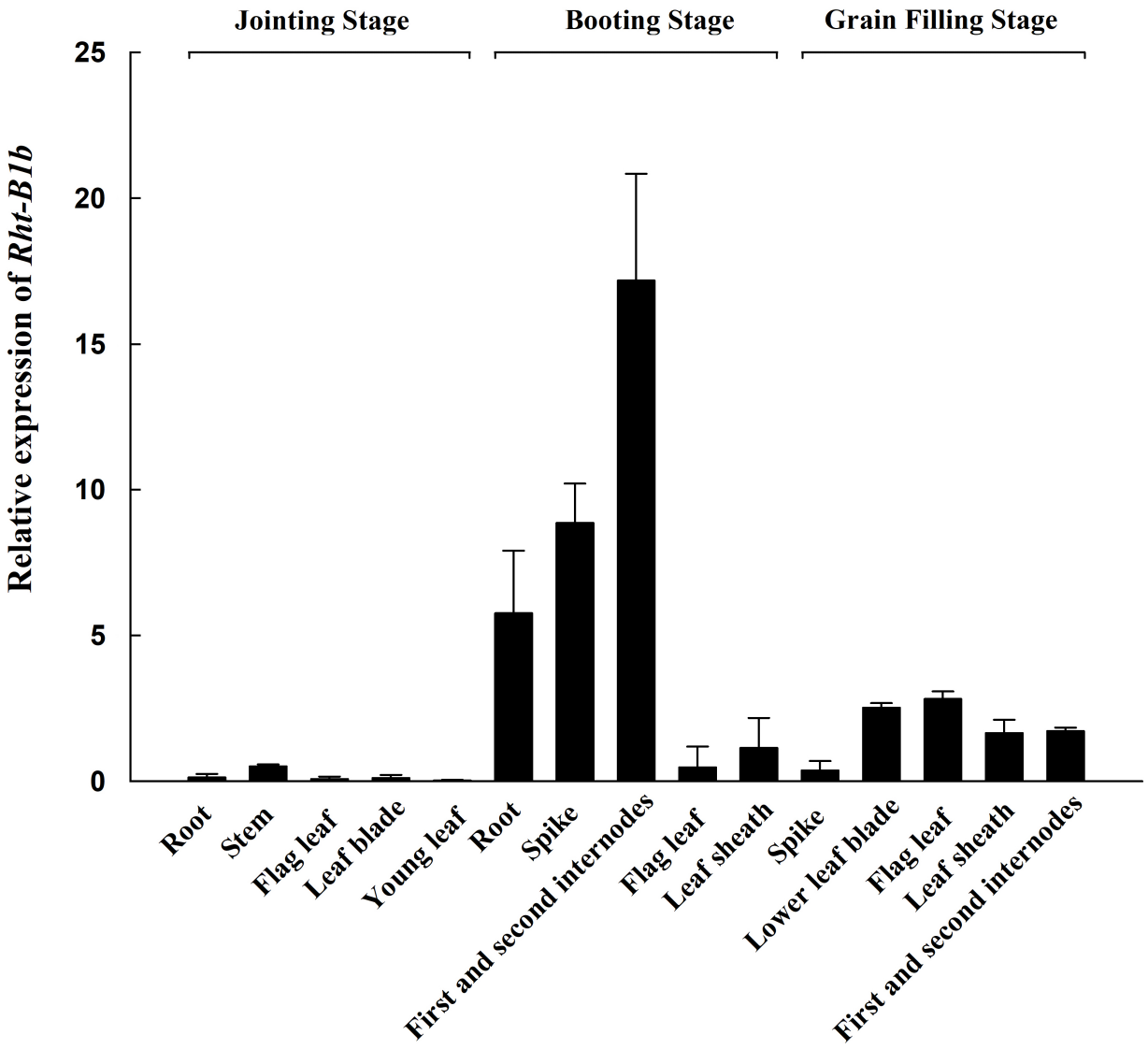


Figure 5

Expression patterns of Rht-dp in various wheat tissues at jointing, booting, and grain filling stages.

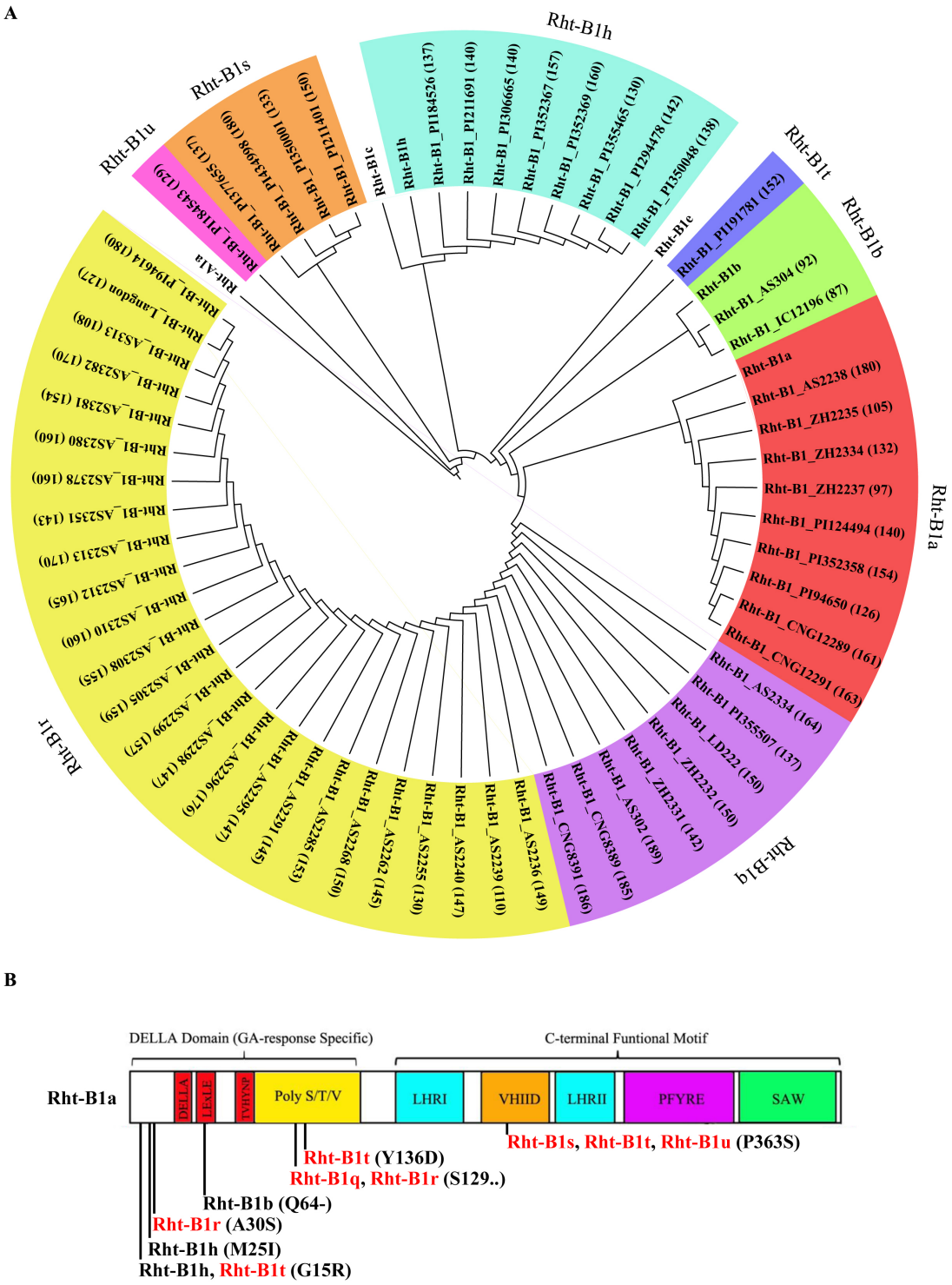


Figure 6

Haplotype analysis of Rht-B1 in 59 tetraploid wheat accessions. A: phylogenetic relationship of Rht-B1 alleles; B: nonsynonymous mutations in Rht-B1.

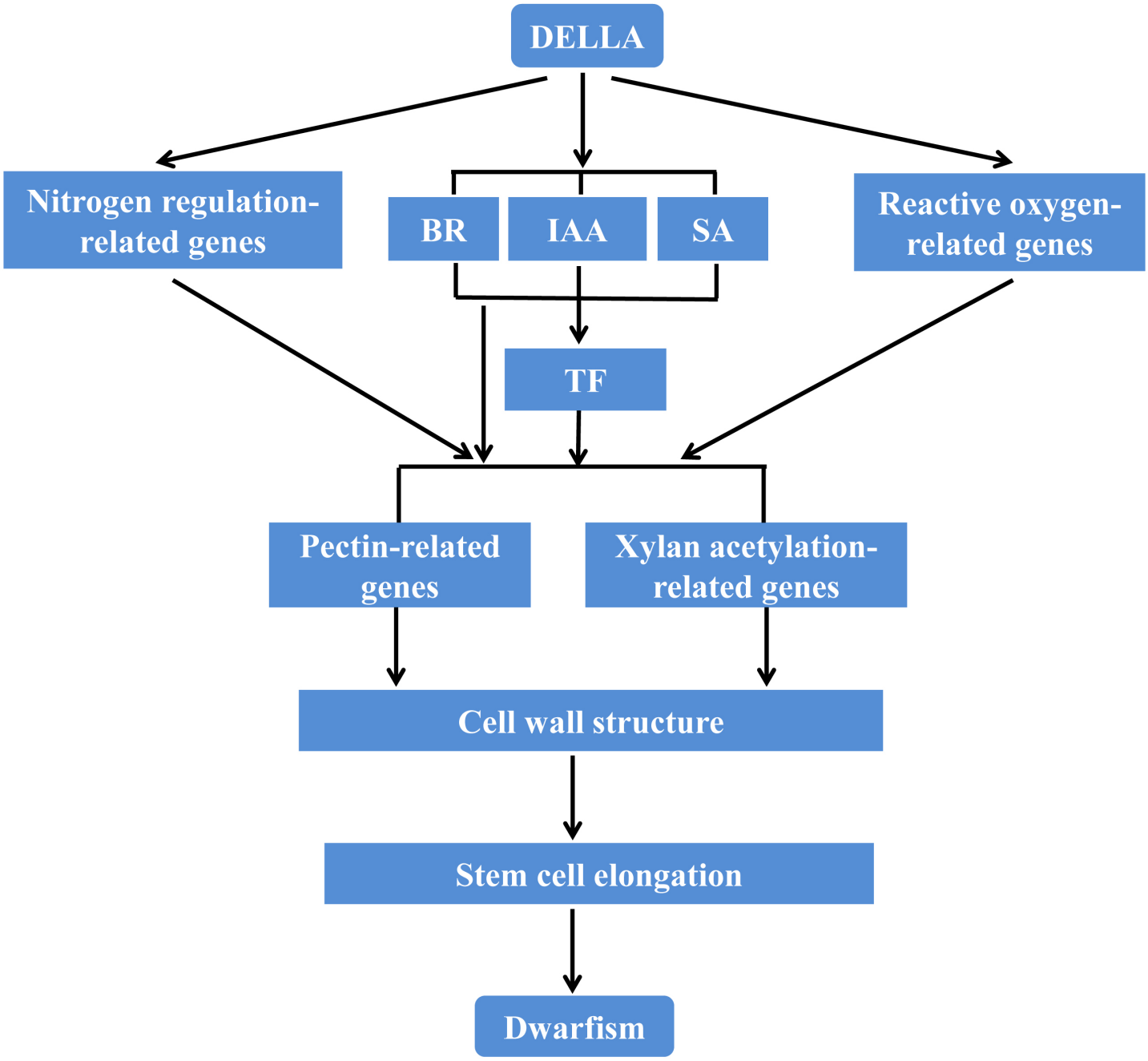


Figure 7

Molecular network model of the DELLA mutation Rht-dp in DPW.

Supplementary Files

This is a list of supplementary files associated with this preprint. Click to download.

- Fig.S1.tif

- Fig.S2.tif
- TableS1.pdf
- TableS2.pdf
- TableS3.xlsx
- TableS4.pdf
- TableS5.xlsx